Title

Helical coiled nucleosome chromosome architectures during cell cycle progression.

Journal

Proceedings of the National Academy of Sciences, 121(43)

Authors

McDonald, Angus
Murre, Cornelis
Sedat, John

Publication Date

2024-10-22

DOI

10.1073/pnas.2410584121

Peer reviewed

PNAS RESEARCH ARTICLE | BIOPHYSICS AND COMPUTATIONAL BIOLOGY OPEN ACCESS

Helical coiled nucleosome chromosome architectures during cell cycle progression

Angus McDonald[a], Cornelis Murre[b], and John W. Sedat[c,1]

Contributed by John W. Sedat; received May 30, 2024; accepted September 4, 2024; reviewed by Karolin Luger and Robert H. Singer

Recent studies showed an interphase chromosome architecture—a specific coiled nucleosome structure—derived from cryopreserved EM tomograms, and dispersed throughout the nucleus. The images were computationally processed to fill in the missing wedges of data caused by incomplete tomographic tilts. The resulting structures increased z-resolution enabling an extension of the proposed architecture to that of mitotic chromosomes. Here, we provide additional insights into the chromosome architecture that was recently published [M. Elbaum et al., *Proc. Natl. Acad. Sci. U.S.A.* 119, e2119101119 (2022)]. We build on the defined chromosomes time-dependent structures in an effort to probe their dynamics. Variants of the coiled chromosome structures, possibly further defining specific regions, are discussed. We propose, based on generalized specific uncoiling of mitotic chromosomes in telophase, large-scale reorganization of interphase chromosomes. Chromosome territories, organized as micron-sized small patches, are constructed, satisfying complex volume considerations. Finally, we unveiled the structures of replicated coiled chromosomes, still attached to centromeres, as part of chromosome architecture.

nuclear structure | chromosome architecture | computer modeling

Significance

This study places all 46 sequenced human chromosomes—correctly filled with nucleosomes and in micron-sized chromosome territories—into 10-micron(average sized) nuclei. The chromosome architecture used a helical nucleosome coiled structure discerned from cryo-EM tomography. This chromosome architecture was further modeled to dynamic structures, structure variations and chromosome replication centromere complications. Finally, this chromosome architecture was modified to allow seamless transition through the cell cycle.

The dominant current paradigm for interphase chromosome structure within the nucleus is a flexible polymer-based system, following polymer statistics [(1–6) and refs therein]. Nevertheless, there is a degree of order as high-throughput DNA sequencing of chromosome conformation captured chromatin has shown [(7–9) and refs therein]. In addition, the relatively specific site associations can be linked to genetic function and control, including during cell type specification and development (10–12).

An alternative depiction of the interphase chromosome structure can be derived from cryo-EM studies. The cell with its nucleus is rapidly frozen, at liquid nitrogen temperatures, to a glassy ice, preserving the interior proteins, nucleic acids, membranes, and water (13–17). The EM data are computer processed, using deconvolution methodology to fill-in the missing high angle data coming from the incomplete tilts (18, 19). The increased Z resolution together with three-dimensional visualization, as stereo rocking movies, now allows insights into the preserved dense nuclear interior [https://doi.org/10.1073/pnas.2119101119, (20)]. These studies indicated that interphase chromosomes fold into an ∼200 nm diameter helically coiled nucleosome fiber, termed a Slinky [defined as interphase S (20, 21). Euchromatin-transcribed sequences appear to be extended interphase S, while heterochromatin folds into a more compact interphase S structure (20). Subsequent studies proposed an architecture for prophase and mitotic chromosomes, as modifications of additional coiling processes [https://doi.org/10.1073/pnas.2119107119, (22)]. The prophase structure is now termed prophase S′, with mitotic chromosome architecture as mitotic S″.

Fundamental to interphase chromosome structure as well as prophase and mitotic chromosomes are constraints, particularly dimensional constraints that are taken from the chromosome and cell biology literature. We examined human chromosomes as a model system. All 46 chromosomes are fully DNA sequenced (23). Since approximately 90% of the DNA is structured as nucleosomes (24, 25), with one nucleosome per 200 base pairs, likely organized as an 11 nm nucleosome fiber, each chromosome will have an essentially defined nucleosome total (Table 1). The essentially complete filling of a given chromosome DNA length with nucleosomes as described above has to be qualified. This result comes from an analysis of nucleosome packing in rat liver nuclei. It is possible that other specific cell types will have less nucleosome density (23, 25). The interphase chromosomes have to fit, as micron-sized chromosome territories, into a nucleus of about 10 microns diameter. Likewise, mitotic chromosomes have dimensions observed from mitotic chromosome spreads (26–29). These boundary limits will restrict what architectures are possible, as were used in the proposed human mitotic chromosome 10 structure (22).

Author affiliations: [a]Micron School of Materials Science and Engineering, Boise State University, Boise, ID 83725-2090; [b]Division of Biological Sciences, University of California San Diego, La Jolla, CA 92093; and [c]Department of Biochemistry and Biophysics, University of California, San Francisco, CA 94158

Author contributions: A.M., C.M., and J.W.S. designed research; performed research; and wrote the paper.

Reviewers: K.L., University of Colorado, Boulder; and R.H.S., Albert Einstein College of Medicine.

The authors declare no competing interest.

[1]To whom correspondence may be addressed. Email: sedat@msg.ucsf.edu.

Published October 14, 2024.

Table 1. The numbered human chromosomes, sequenced length in base pairs, number of nucleosomes/lengths, the S interphase length, and Ch. Terr. Vol. are shown in Table 1

Chromosome	Base pairs ($\times 10^8$)	Nucleosomes ($\times 10^6$)	S interphase length (Microns)	Ch. Terr. Volume (Microns^3)
1	2.484	1.081	196.5	17.05
2	2.427	1.056	192.0	17.28
3	2.011	0.875	159.1	13.80
4	1.936	0.842	153.1	13.28
5	1.821	0.792	144.0	12.49
6	1.721	0.749	136.2	11.81
7	1.606	0.699	127.1	11.02
8	1.463	0.636	115.6	10.03
9	1.506	0.655	119.1	10.33
10	1.348	0.585	106.4	9.23
11	1.351	0.588	106.9	9.27
12	1.333	0.580	105.5	9.15
13	1.136	0.494	89.8	7.79
14	1.011	0.440	80.0	6.94
15	0.9975	0.434	78.9	6.84
16	0.9633	0.419	76.2	6.61
17	0.8428	0.367	66.7	5.79
18	0.8054	0.350	63.6	5.52
19	0.6171	0.268	48.7	4.23
20	0.6621	0.288	52.4	4.54
21	0.4509	0.196	35.6	3.09
22	0.5132	0.223	40.5	3.52
23 (X)	1.5426	0.671	122.0	10.58

Recent Kinetic Extensions of Interphase S, Prophase S′, and Mitotic S″ Chromosome Structures

We extend the analysis of the coiled chromosome structures described in our recent studies (20, 22). The Slinky structures, interphase S, prophase S′, and mitotic S″, are now built as a time series showing these structures coiling (Fig. 1). We use engineering coiling software (30), suitable modified, described in detail in *Methods and Materials*, so that the correctly dimensioned molecular outline of the nucleosomes structures is shown; this approach was used in previous studies (20, 22). This time series allows one to search for difficult building and/or formation points, including kinks, compression points, or abrupt bends in dynamic coiling. Study of the kinetic data suggests a smooth construction series without obvious problems (Fig. 1), though additional kinetic studies using faster coiling, for example, might reveal other issues or problems. By monitoring the kinetics displayed by movies in a backward manner, we were able to visualize interphase S structure pulling apart [analogous to pulling a Slinky (21) apart to different degrees] during the course of nascent transcription. This was proposed and outlined in detail in figures 3 and 4 in ref. 20.

One of the main reasons for developing the kinetic series is a proposal to use the time series to intersect with FEA (31, 32), the detailed modern physics quantitation and analysis approach. With this methodology, it is possible to determine fundamental forces and estimate diffusion parameters in solvents of suitable viscosity. Could bending, coiling forces, and forces required to pull the interphase S gyri apart for transcription be determined? What are the forces to indent and distort the prophase S and mitotic S′ gyri?

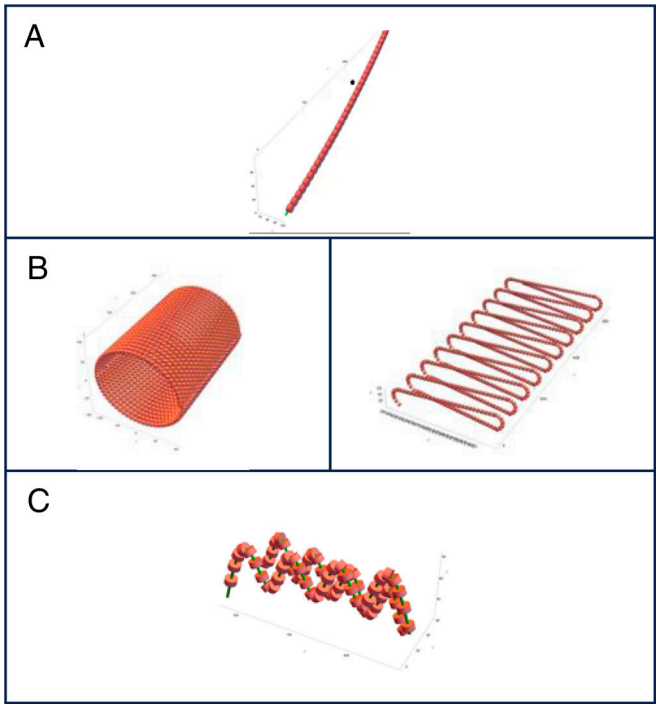

Fig. 1. A unified chromosome architecture based on multiple helical structure coiling as a dynamic process. Panel *A* shows the helical coiling of the 11 nm nucleosome fiber into the interphase chromosome, termed interphase S, a structure extensively described in ref. 20. This figure emphasizes the coiling dynamics as clickable/link movies activated by clicking on the Fig. 1*A*, and the coiling controlled by the movie bar(red) left-to-right for coiling and right-to-left for uncoiling (note the right-hand side of the movie bar controls sound, not used). The more open coiling, initially, and later the pulled-out coils emphasize the transcription process, while the more compressed coiling is likely heterochromatin structure, best seen in *B*. Note that enlarged views of the movies are possible by clicking the enlargement button. Some practice, playing the movies, shows additional features of the dynamics. Panel *B* shows the further modifications of the interphase S structure, seen in panel *A*, to form prophase chromosome structures (prophase S′). The *Left* side of panel *B* first compresses the interphase S gyri to form a flattened structure, and on the *Right* side of the panel indentations (like an accordion), on both sides of the flattened surface, are inserted. Again, the movies are played by clicking on the Fig. 1*B Left* and Fig. 1*B Right* This structure is described in detail in ref. 22. Panel *C* shows the helical coiling of the prophase chromosome structure, from panel *B*, to form a mitotic chromosome (mitotic S″), as detailed in ref. 22. Clicking on the Fig. 1*C* activates the movie. A summary and point for Fig. 1. The essential movies show the coiling of the 11 nm nucleosome fiber—its structure—as well as the coiling architecture described in ref. 20 makes the point that additional modifications for prophase and the further coiling for mitotic chromosomes build all chromosome states, as brought out by the movies. Makes the point that the dynamics, seen in the movies, set up further polymer physics quantitation and finite element analysis (FEA) studies.

What forces are required to coil the mitotic S″ structure in the final mitotic helical winding? Could handedness preference, at the different levels of coiling, be investigated? The FEA approach should yield physics-based data that can be linked to biochemical study for the investigation of nuclear and chromosome structure. Experimental data from optical and Cryo-EM tomography should intersect with the FEA approach and is essential to achieve a deeper understanding of chromosome structure.

It should be noted that there are several ways to coil structures; the approach described above emphasizes search for coiling problems and a possible link to the proposed FEA direction. Another coiling paradigm, coiling an entire intact built structure, with time points, is described in Fig. 3.

Structure Variations for Interphase, Prophase, and Mitotic Chromosomes. Structural variations, are seen throughout interphase S, prophase S′, and mitotic S″ chromosomes (20 and 22)

and shown in detail in Fig. 2. We found that the diameter of the interphase S fiber fluctuates around an average value of 200 nm but spanning distances of 100 to 300 nm (20) (Fig. 2). In addition, we detected many instances of indentations of the diameter of the helix (Fig. 2*D*). A prominent example of such indentations and variations is shown in a drawing of an interphase chromosome revealing the many surface variations resulting from the interphase S diameter distinctions (Fig. 2*E*). We predict the presence of regions of interphase S regions that are depleted for nucleosomes that span regulatory elements including promoters and enhancer regions (33–37), and thus, these depleted regions could account for some variations. The interphase S structure is likely, especially in light microscope studies, to give the appearance of clumps of structure; transcription regions will be variably pulled out, while other regions, less or not transcribed, will be more compact. Prophase S′ dimension variations, where the X axis can be extended slightly, broadened, by modulation of the indentations of the flattened prophase S′ gyri are readily revealed (Fig. 2 *F* and *G*). The prophase S′ width variants are further coiled to assemble mitotic chromosome resulting in mitotic S″ helical coiling (Fig. 2 *H* and *I*). Mitotic S helical coiling resulted in an increase in the outside diameter of the mitotic coil but did not reveal changes in the inside diameter dimensions (Fig. 2*H*). We note that the consequence of this variation is the appearance of outside mitotic chromosome surfaces, in chromosome spreads, as bumpy/rough—many small ridges arranged roughly at 90° to the chromosome long axis—because of the diameter variations (see refs. 26–29). A possible rationale for the structure variations is analyzed in *Discussion*.

A Proposal for Interphase S, Prophase S, and Mitotic S″ as Unified Chromosomes Structures throughout the Cell Cycle. The fundamental architecture of chromosomes must allow, in a seamless fashion, the dramatic changes in their overall structure to take place during the cell cycle: condensation in prophase to form the mitotic chromosome structure and decondensation in telophase as the interphase chromosomes/ nucleus reforms. As a first approach to understanding this change in chromosome structure, we modeled human chromosome 21, the smallest human autosome (45 million base pairs long with 196,000 nucleosomes, Table 1), as a plausible architectural route through the cell cycle (Fig. 3). Starting in interphase (G1) for this specific human chromosome, chromosome 21, the interphase S also folds into 14 micron sized large-scale coils (Fig. 3*A* and legend). We conjecture that all interphase S structures are associated with large-scale loops, plausibly involving megaloops as a fundamental aspect of their structure. Here, we define such loops as "Primordial Coils." Prophase S′ shows prophase chromosomes, now condensed

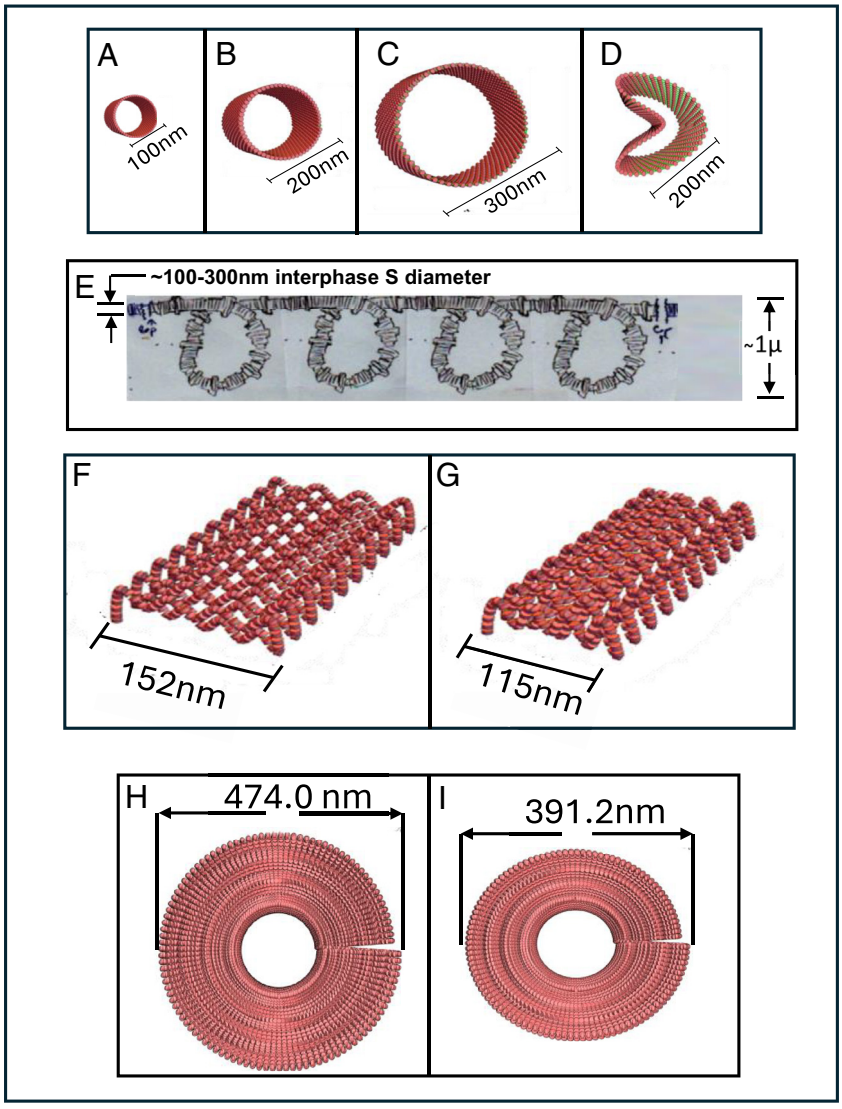

Fig. 2. Structure variations are seen at every level of the helical coiling architecture. Fig. 2 shows variation of the interphase helix (interphase S) diameter seen and documented in ref. 20. Panel *A* shows a 100 nm diameter, the middle, *B*, the most common 200 nm diameter, followed by examples of 300 nm diameter dimensions (*C*). The *Right* side panel *D* shows that the helix diameters were frequently misshapen and indented. Just underneath, *E*, is a free-hand drawing of an interphase chromosome (interphase S) region, with dimensions, where these variations would result in rough, not smooth, overall surface. Panels *F* and *G* show that the prophase chromosome structure (prophase S′) also had variations, primarily variations in the size of the pleats/indentations, which creates wider or more narrow X axis structure. Panels *H* and *I* show that the mitotic chromosome coiling (mitotic S″ using the additional coiling) would have mitotic diameter variations because different sized prophase variants were used to coil. The left side coiling used the prophase chromosome dimensioned from the *Left* side of *F*, while the right side used the prophase chromosome of *G*. Note, while the mitotic diameter varies, the inside diameter is constant. A summary and point for Fig. 2 make the point that each of the Slinky based chromosome structures are not uniform (or monolithic) but have variations that modify the final structures.

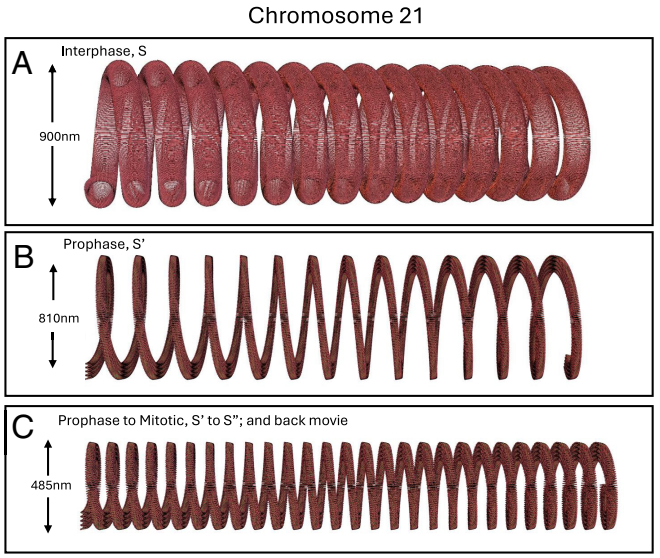

Fig. 3. A unified hierarchical coiled chromosome architecture transits through the cell cycle, as depicted for human chromosome 21. Panel *A* depicts chromosome 21 as an interphase structure with 14 approximately 1-micron-large coiled loops (the Primordial Coils described in the text). These coils resulted from a partial specific uncoiling of the mitotic chromosome in telophase (see panel *C*); the Primordial Coils to emphasize their organizational relationship in the cell cycle; these coils were the basis of chromosome territories described in Fig. 4. Below the level of the Primordial Coils is the interphase chromosome structure, helically coiled structure of the nucleosome 11 nm fiber, interphase S, extensively described in ref. 20 and Fig. 1. Panel *B* depicts chromosome 21 as a prophase chromosome structure, a compressed and pleated structure (prophase S′), described in ref. 22 and Fig. 1. In prophase, this prophase chromosome has the same locations and numbers of Primordial Coils (14, 1 micron) resulting from the telophase mitotic chromosome unwinding. Panel *C* is a movie [clickable on the Fig. 3*C* as described in Fig. 1] depicting the further compaction of chromosome 21 from a prophase structure (the first frames of the movie). The movie shows the prophase structure coiling into a chromosome 21 mitotic chromosome—forming the tighter 0.5 micron mitotic coils. The mitotic chromosome architecture was described in ref. 22 and Fig. 1. It can be seen that two mitotic coils form for each Primordial Coil forming the tighter 0.5 micron mitotic coils, and 28 final mitotic coils. It can be pointed out that the mitotic chromosome for chromosome 21, seen here, is slightly extended to emphasize the coiling, if compressed a correct sized chromosome 21 would result (22). Panel *C* also shows the telophase chromosome structure as part of this phase of the cell cycle. The movie is just played in reverse; the movie bar is now moved right-to-left and chromosome 21 unwinds specifically two mitotic coils for every Primordial Coils, recapitulating what one sees for prophase and interphase. Initially, this unwinding of the mitotic chromosome is a prophase structure, which rapidly turns into an interphase structure. Going from *C* to *A* suggests that the cell cycle has nested coiling-architectural features that allow the chromosome to process through the cell cycle seamlessly. A summary and point for Fig. 3 makes the point that the sequentially coiled chromosome structures can decondense in defined ways so that they can go seamlessly through the cell cycle. The mitotic chromosome coiled (human chromosome 21), as described in ref. 22, uncoil in specific ways, in telophase, to give rise to large-scale 1-micron interphase S(Slinky) coils, ready to build chromosome territories. The movie brings out the specific uncoiling. This is a different way to see the transition through the cell cycle.

as described (22), but with the same number and spacing as the Primordial Coils in interphase S (Fig. 3*B*). Highlighting the assembly of mitotic chromosomes, by visualization (Fig. 3*C*, movie), readily reveals the dynamics of mitotic chromosomes coiling. Specifically, we conjecture that mitotic coiling created two tighter mitotic coils (about 500 nm in diameter) for every Primordial Coil, for a total of 28 mitotic coils just as we modeled, with the proposed architecture, human mitotic chromosome 10 in ref. 22. Played backward, the movie highlights telophase. We propose that in telophase, mitotic chromosomes uncoil discontinuously. Some spaced coils remain—possibly two adjacent mitotic coils fused to create micron size Primordial Coils. Such Primordial Coils remain in interphase/G1 to instruct the assembly of chromosome territories (Fig. 4 *A*–*D*). Thus, these observations indicate that special coils—Primordial Coils—build features that architecturally are ready to proceed to the next step in the cell cycle. A key aspect of the interphase S structures is that they remain as coiled nucleosomes fibers throughout the entire cell cycle and never require disassembly using this architecture.

Interphase S Chromosomes as Chromosome Territories. Interphase chromosomes are not intertwined randomly in the nucleus but occupy distinct regions known as chromosome territories (38–41). The chromosomes in most organisms that have been examined are arranged in the Rabl configuration (named after the 19th-century cytologist Carl Rabl), in which the centrosomes cluster at one side of the nuclear envelope and the telomeres are attached to the opposite side, a consequence of chromosome segregation at anaphase (42–47). We recently built an interphase S chromosome as a Rabl chromosome territory (20).

Higher eukaryotic genomes are segregated into many individual chromosomes and organize their chromosome territories not as Rabl structures but as micron-sized patches (see especially the figure in ref. 39). Initially, we suggest a framework for chromosome territories. This framework is a series of approximately 1-micron Primordial Coils (Fig. 3). These Primordial Coils are straightened then tightened to make an approximately micron-sized patch (Fig. 4 *A*–*C*). Human chromosome 19 is the representative example for the structure of the patch-sized chromosome territory (Fig. 4 *A*–*C*). Visualization reveals possible kinetics that underpins the assembly of chromosome 19 into a chromosome territory (Fig. 4*D*, movie). We also modeled the chromosome territory of human chromosome 21 and show how it fits into a correctly scaled 10-μm-diameter nucleus (Fig. 4 *E* and *F*)

All 46 human chromosomes, as patch chromosome territories, have to fit into a 10-micron (average size) nucleus. Using chromosome 19 as a volume template for a chromosome territory, and the 46 chromosomes (calculated as nucleosomes/chromosome) allows possible scaling of the chromosome territories (Table 1). The chromosome territories sizes, located in Table 1, column 5, are summed together (times two for the other homologs); it was possible to show that all 46 chromosomes fill a 10-micron nucleus at the 80.29% volume level. This is likely an upper limit as we assumed cubic chromosome territory volumes (Fig. 4 *A*–*C*). This result suggests that interphase S architecture is compatible with patch-based chromosome territories. Given the remaining 20% (or more) volume in the 10-micron nucleus, we expect that there will be freedom to uncoil/distribute the chromosome territories in more open configurations, for example, to enable interphase S for transcription. Chromosome motion should expand/unfold somewhat the chromosome territories. We emphasize that the patch chromosome territory, as built here, is a model for that assembly of chromosome territories, but that other chromosome territory models are plausible.

The individual chromosome territories in our model are quite dense appearing. Study shows significant space in the turn-around regions of the straightened large-scale micron-sized Primordial Coils as seen in the movie of Fig. 4*D*, as well as the interiors of the interphase S structure. For reference, chromosome 19 contains 268,000 nucleosomes (Table 1) in a patch that spans approximately 4 microns^3. Such a configuration should permit the assembly of topologically associating domains (TADs), as regions are close together. Indeed, in our STEM Cryo-EM Tomography images, we noticed several side-by-side parallel associations of interphase S regions (20). Moreover, live cell imaging studies revealed predominantly intrachromosomal loop associations rather than interchromosomal interactions (42).

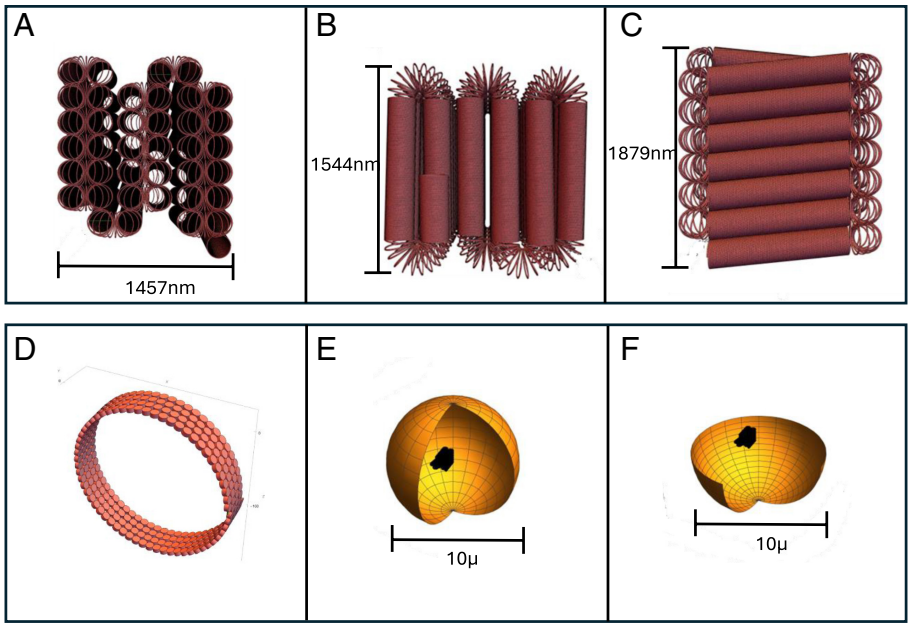

Fig. 4. The helical coiling architecture is used to construct higher eukaryote micron-sized chromosome territories. Panels *A–C* depict human chromosome 19 constructed as human chromosome territory, in X, Y, and Z views with dimensions. A chromosome territory is built by using its interphase chromosome 1-micron loose Primordial Coils left over from specific unwinding, in telophase, of the mitotic chromosome. These loose micron sized coils are flattened to reduce space with further compaction to make chromosome territories. The micron loops are further defined in Fig. 3; however, they show that the residual telophase mitotic chromosome unwinding is used architecturally for chromosome territories. Panel *D* shows a movie [click on the Fig. 4*D*] of the construction/organization of chromosome 19 chromosome territory. Panels *E* and *F* depict chromosome 21, as another example chromosome territory, as one homolog, correctly dimensioned, in a 10-micron (average size) nucleus diameter. A summary and point for Fig. 4 makes the point that a micron-sized chromosome territory, using human chromosome 19, can be made, an undocumented result in the literature. The movie shows how the large-scale 1-micron coils sets up the formation of the chromosome territories. This micron size chromosome territory structure is extended in the text to further show that all 46 human chromosomes fit as chromosome territories, at the 80% volume level, in an average sized 10-micron diameter nucleus.

Implications for DNA Replication Involving Interphase S, Prophase S′, and Mitotic S″ Chromosomes. Any chromosome architecture has to take into account the impact of DNA replication (48–51). We show that after replication the two interphase S structures interdigitate-nest-inside each other, a natural feature for Slinky architecture (Fig. 5*A*). Upon replication completion, the two interphase S structures could slide out from each other, likely still positioned within close spatial proximity from one another. Another important feature of the nested interphase S Slinky structure is that they are able to rotate about the long axis of the helix allowing structural flexibility. We note that it is conceivable that strand separation occurs at the start of G2/prophase or alternatively that it is discontinuous because of replication timing.

A sight complication is seen at centromeres (56). We hypothesize that the replicated centromere DNA interphase S structures still interdigitate/nest and held together by cohesin (52–55) (Fig. 5*B*). It is plausible that late DNA replication of the centromere may play a role in this process.

The separated replicated interphase S chromosomes are free to form prophase chromosomes, as prophase S′, at the right time in the cell cycle, as shown in Fig. 5*C*. Again, the slight complication is the centromere region; centromeres remain likely uncondensed as interphase S, interdigitated/nested together, held tightly by cohesin protein (52–55), and diagrammed in Fig. 5 *C*, *Inset*.

Mitotic chromosomes coil as part of the mitotic S″ coiling, with the replicated sister chromosomes side by side shown in Fig. 5*D*. Also, there is the centromere complication; the two sister centromeres are still in interphase S, coiled, interdigitated/nested together (Fig. 5 *D*, *Inset*). The key point is that the centromere, in interphase S, is not further coiled to prophase S′ or mitotic S", and the sister chromosomes, held together by cohesin protein, associate as a pair as seen in the chromosome spreads (26–29). Mitosis takes place with the attached mitotic chromosomes, a lengthy process (49, 57), until at anaphase cohesin is cleaved to release the two sister chromosomes (52–55).

Discussion

Coiling Aspect. Coiling helically, in some cases sequentially, seems to be a paradigm that is used over and over again to describe folding patterns for DNA structures. For example, DNA folds as a right-handed two-strand-helically coiled structure. The nucleosome is organized as a discontinuous left-handed coiled structure that is folded around the octamer histone core (58). Helically coiling involving the nucleosome 11 nm fiber, in turn, assembles into an interphase S structure. A proposal, in a previous paper, showed that polytene chromosomes, a representative—with higher-order structure, interphase chromosome(G1/S)—could be built with coiling features of the interphase S structure(discussed in ref. 20). Prophase S′ is modified interphase S, still with its coiling, and this could be extended to lampbrush prophase I chromosome structure as an example (20). Helically coiling prophase S′ to make mitotic S″ (hand unspecified) along the same line follows the coiling paradigm. How is it possible to coil this plethora of structures, and which enzymes/proteins are required? These are important study directions.

We recently showed that condensin, which functions in chromosome condensation and segregation in mitosis and meiosis (59, 60), with just the right molecular spacing, was possibly involved in the assembly of prophase S′ topologies (20). Prophase S′, as built and displayed, involved a two-step process, because the software for the correct molecular and structure simulations was somewhat inflexible. Prophase S′ could be envisioned, in vivo, as a much simpler, possibly enzymatic/protein problem. In interphase S, on each side of the interphase S gyri at eight separate spaced points—four points at the top and four points at the

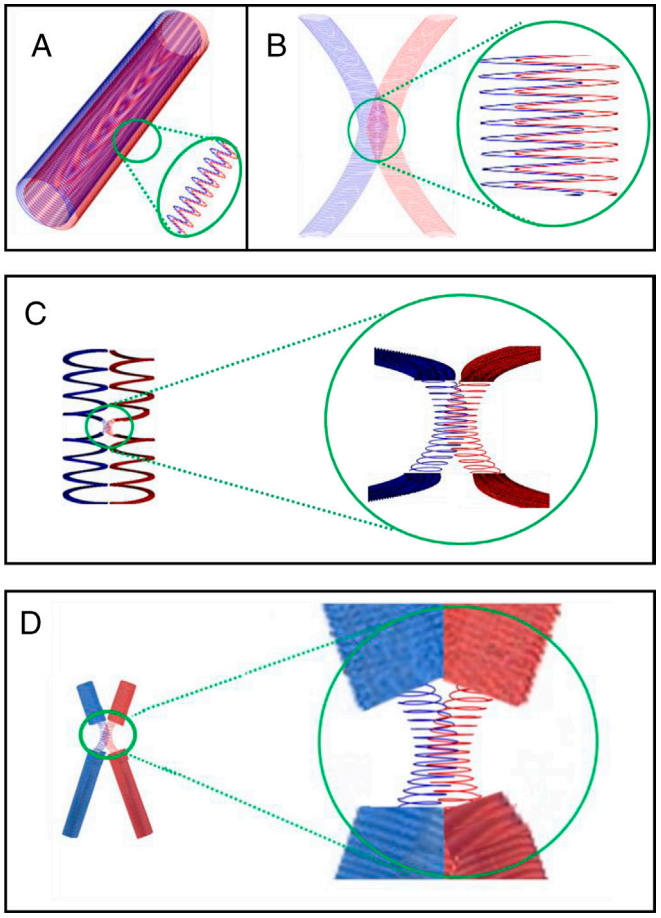

Fig. 5. Helical coiled architecture as a function of chromosome replication. Panel *A* depicts, as line drawing, two interphase (interphase S) replicated chromosomes, blue line for the original, and red line for the replicated interphase chromosome; just after replication the two chromosomes are nested, a natural Slinky helix process—inside one another as the *Inset* shows. The *Inset* is an enlarged view of the nesting. After replication, the two replicated helices just slide out from each other, seamlessly, as seen in *B*. Panel *B* shows that the centromeres are treated differently; they continue to be interdigitated because they are held together by cohesin protein (52–55). Panel *C* shows prophase replicated chromosomes, blue for original and red for replicated, fully separated except for the centromere. These still are held together by cohesin and interdigitated. Note that the centromere region is still an interphase S structure. Panel *D* shows replicated mitotic chromosomes still held together by the cohesion-mediated interdigitation of the centromere region, still as an interphase S structure, until anaphase where the cohesin enzymatically is degraded and releases the sister mitotic chromosomes (57). These are accurate human chromosome 10 (23), except for the centromere regions. A summary and point for Fig. 5 makes the point that replicated interphase chromosomes are nested Slinky (interphase S) Structures. Subsequent cell cycle chromosome stages continue to nest the centromere chromosome regions, held together by cohesin protein. In anaphase, the cohesin protein is degraded, allowing the nested centromere regions to separate. Explains the mitotic chromosome structure centromere gap seen in mitotic chromosome spreads.

bottom of the gyrus—could be identified and then pulled using possibly concatenated condensin to both collapse the interphase S gyrus into a race-track configuration associated with deep indentations (Fig. 1*B*) (59, 60).

Interphase S Polymer Considerations. We emphasize that interphase S, the interphase chromosome architecture, is in essence a special polymer structure that is folded into an approximately 200 nm diameter coiled, hollow, and flexible Slinky. It is likely to follow, polymer statistics (1–6, 61, 62), though special attributes apply, especially since this is a densely coiled structure with special features. For example, in one axis, interphase S is very easily bent and deformed, while in the other directions, the interphase S gyri compress restricting bending. How the polymer dynamics are affected is an interesting question and complicated by the very high density of nucleosomes, in some cases akin to that of chromosome territories chromosomes. In addition, the somewhat small 10-micron nucleus, constrain the chromosomes, the well-known "cage or box" effect (62). The close edges restrict diffusion and change polymer statistics. In summary, the interphase S architecture, overall, has many features in common to the polymer-based systems, physics, and thinking the community and literature currently considers (1–6, 61, 62).

There are several attributes to consider for interphase S structures. First, interphase S are dense coils that are predominantly perpendicular to the interphase S long axis and are very densely packed (approximately 64 nucleosomes-12.8 kb/gyrus). Second, interphase S are hollow, and when pulled out almost free diffusion of the hollow interior compared to the interphase S exterior; if interphase S is compressed as it is for heterochromatin, the hollow interphase S interior would have restricted diffusion, possibly used for protein storage or a different enzymology. Third, interphase S structures can be straight for regions and the closely packed interphase S gyri could associate one gyrus with another giving rise, possibly to better rigidity (20). Fourth, we note that the exterior surface of interphase S is extended compared to the hollow interior, and long-range 2-dimensional aligned phased nucleosome interactions are possible (20, 22). It is conceivable that this would enable increased cooperative interactions involving chromosomal-associating proteins (63, 64). Fifth, interphase S allows for adjacent interphase S coil nesting interactions as pointed out in the interphase S replication and centromere adhesion situations. TAD interactions could make use of such an interphase S feature. Sixth, interphase S structures could well allow for genetic coordination by epigenetic marks on adjacent interphase S gyri. Seventh, it is conceivable that such a delicate interphase S structure is potentially sensitive to fixation making it difficult to interpret structural information derived, for example, from formaldehyde-fixed cells.

Structure Determination Aspects. A major point to make is that additional experimental data are urgently needed. While there is now Cryo-EM interphase chromosome structure data (20), the detailed experimental data/structures for prophase S′ or mitotic S″ chromosomes are not existent, just a proposal for the structures (22). The right experimental system, we feel, is cryo-EM Tomography, since the structures are likely faithfully preserved in a glassy frozen aqueous state. Recent progress in STEM EM technology will allow even better data collection and computer processing; double tilts, on an orthogonal axis, followed by deconvolution show improved Z resolution; better filling of the missing wedge coming from incomplete high-angle tilts information (65). Recent detector technology now provides fast 96×96 pixels at 120,000 frames per sec. data collection, possibly allowing increased contrast or possible specific atom detection (like Nitrogen for nucleic acid/DNA, for example ref. 65).

Detailed three-dimensional optical microscopy will also greatly help prophase S′ and mitotic S″ structure determination. In this regard, the polarization microscopy/birefringence optical studies of nuclei, suggesting ordered structures, may need to be reexamined; the nuclear substructure, never interpreted or understood (66), is reminiscent of the interphase S architecture described in ref. 20.

Variability in Interphase S, Prophase S′, and Mitotic S″ Structures. Since it is possible to vary each of the interphase S, prophase S′, and mitotic S″ structures, one could ask why does such a degree of variation exist. Is this variation used to distinguish

specific genetic regions from one another involving differences in transcription timing or regulation? One hypothesis comes from observations made in *Drosophila melanogaster*. All 5,000 polytene bands are structured into distinctive shapes and sizes (67). Recent studies showed that polytene bands are folded as TADs (the same as diploid interphase chromosomes) and are composed of tissue distinctive regulatory elements (68, 69). Hence, we conjecture that interphase S variations consist of DNA elements with distinct regulatory functions (70). We again emphasize that polytene chromosomes are examples of bonified interphase chromosome structure (67–70).

Interphase S Replication Aspects. DNA replication process suggests that the interphase S architecture facilitates replication segregation and possible control of the replication events (Fig. 3). The centromere on mitotic chromosomes, for example, on metacentric chromosomes, is a constriction, compatible with interphase S structure. The centromere adhesion for prophase and mitotic chromosomes was an old problem, with a suggested molecular solution.

Homolog Chromosome Considerations. An important experimental result showing restricted nuclear chromosome localization needs discussion. Hua and Mikawa documented that in low-passage human primary cells (but not cancer cell lines), the two homologs are restricted to separate halves of the nucleus, not intermixed, at least during early metaphase and anaphase (71). A recent study provides evidence that chromosome centromere markers components are separated by a deep cleft in the middle of the metaphase chromosome mass along the centrosome axis of the nucleus, suggesting restriction of homologs in significant phases of the cell cycle, with little or no mixing of homologous chromosomes (72).

Conclusions. In conclusion, we note that a Slinky-based architecture is able to withstand potential complications-kinetics, structure variants, flow through the cell cycle, micron patch chromosome territory dimensions and chromosome replication issues, indicative of architectural robustness. However, insights into mechanisms that permit the folding of 2 m of DNA, packed with nucleosomes, into a 10-micron mammalian nucleus and proceed orderly through the cell cycle remain rudimentary and will require further experimentation using both cryo-EM approaches as well as live cell imaging.

Methods and Materials

Computer modeling software, and computer hardware/software utilized for this paper, follows our previous publications (20, 22).

In brief, we adapted the software package of an engineering group that was mathematically modeling, in three-dimensions, sequential coiling of suspension bridge cables (30); this was implemented in Mathematica (73), a gold standard software package for equation/mathematics manipulation. The group showed that FEA (31) could then be made on the bridge cables (30).

Instead of bridge cables, we used their mathematics, with their software, in the computer, to coil DNA, scaled so it was a thin 2 nm line (ignoring the DNA helical coiling). Then, we built nucleosomes scaled as a 11-nm disk with a 5.5 nm thickness attempting to match the molecular outline of the published Lugar et al. crystal structure (58). Then, we attached a correctly dimensioned linker DNA (50 base pairs), for a nucleosome unit, which was further iterated into an 11 nm nucleosome fiber (see ref. 20). Mathematica allows coiling (even sequentially), with bending and twisting, at any scaling, so that the correct dimensions are maintained.

Some of the nucleosome structure packing considerations (whether the nucleosome disks face each other or are at 90° to each other) are detailed in ref. 20. The correctly dimensioned molecular outlines of the nucleosomes can be seen in detail, especially in large enlargements of the chromosome structures (figures 3 and 4 in ref. 20). In the images, in Figs. 1–4, where the whole human chromosomes are shown, the nucleosomes are just very small disks, correctly dimensioned, but with poor resolution due to the large number and dense packing of the nucleosomes.

Our use of Mathematica 14.0 (73) was on both Linux and Microsoft Windows systems. Mathematica 14.0 was run under Windows 11, Intel(R) Core(TM) i7-10700 CPU @ 2.90 GHz 2.90 GHz, with 64.0 GB of ram and displayed on a Samsung C27F591 monitor with a NVIDIA RTX A5000 video card with 24 GB GDDR6 memory. The Linux system ran Mathematica on a CentOS Linux release 7.9 system running on Intel Core i7 CPU 2.80 GHz processor with 16 GB of memory for some processing. The display of the Linux-generated output was visualized on the Windows 11 computer.

The software was modified to take-into-account the time-dependent/kinetic interphase S configuration, prophase S′ modifications, and the mitotic S″ coiling. The movies of the chromosome timeline were all made with Wolfram Mathematica 13.0. Each frame of the movie was generated as a Mathematica Graphics3D figure and stored in an array. The parameters of the Graphics3D command were changed in each frame to reflect the conformational changes of the chromatin structure. Finally, the array of stored frames is converted and stored as to a QuickTime movie using the Mathematica Export command.

The various scripts for the software are supplied by the authors upon request.

Data, Materials, and Software Availability. All study data are included in the main text.

ACKNOWLEDGMENTS. We gratefully acknowledge the advice and suggestions of Professors Thomas Cremer, Christoph Cremer, Geeta Narlikar, Zvi Kam, Lisa Hua, Lloyd Smith, and Marc Shuman. We are grateful for the editing of Carol Featherstone of Life Science Editors. The computing research and computer resources are self-funded by A.M. and J.S. Research in the Murre laboratory is supported by the NIH RO1AI082859, RO1AI082850, and US1-BSF 2019280.

1. N. Khanna *et al.*, Chromosome dynamics near the sol-gel phase transition dictate the timing of remote genomic interactions. *Nat. Commun.* **10**, 2771 (2019), 10.1038/s41467-019-10628-9.
2. J. Lucas *et al.*, 3D trajectories adopted by coding and regulatory DNA elements: First passage times for genomic interactions. *Cell* **158**, 339–352 (2014).
3. X. Lin, B. Zhang, Explicit ion modeling predicts physiochemical interactions for chromatin organization. *eLife* **12**, RP90073 (2023), 10.7554/.90073.1.
4. R. Cheng *et al.*, Exploring chromosomal structural heterogeneity across multiple cell lines. *eLife* **9**, e60312 (2020).
5. M. Di Pierro *et al.*, De novo prediction of human chromosome structures: Epigenetic marking patterns encode genome architecture. *Proc. Natl. Acad. Sci. U.S.A.* **114**, 12126–12131 (2017).
6. G. Forte *et al.*, Bridging condensins mediate compaction of mitotic chromosomes. *J. Cell Biol.* **223**, e202209113 (2024).
7. J. R. Dixon *et al.*, Topological domains in mammalian genomes identified by analysis of chromatin interactions. *Nature* **485**, 376–380 (2012).
8. E. P. Nora *et al.*, Spatial partitioning of the regulatory landscape of the X-inactivation centre. *Nature* **485**, 381–385 (2012).
9. Y. Zhu, M. G. Rosenfeld, Y. Suh, Ultrafine mapping of chromosome conformation at hundred basepair resolution reveals regulatory architecture. *Proc. Natl. Acad. Sci. U.S.A.* **120**, e2313285120 (2023).
10. A. Loda, S. Collombet, E. Heard, Gene regulation in time and space during X-chromosome inactivation. *Nat. Rev. Mol. Cell Biol.* **23**, 231–249 (2022), 10.1038/s41580-021-00438-7.
11. E. Heard, C. Rougeulle, Digging into X chromosome inactivation. *Science (New York, N.Y.)* **374**, 942–943 (2021).
12. F. Dossin, E. Heard, The molecular and nuclear dynamics of X-chromosome inactivation. *Cold Spring Harb. Perspect. Biol.* **14**, a040196 (2021), 10.1101/cshperspect.a040196.
13. M. Elbaum *et al.*, Cryo-scanning transmission electron tomography of biological cells. *MRS Bull.* **41**, 542–548 (2016).
14. P. Kirchweger *et al.*, Visualization of organelles in situ by cryo-STEM tomography. *J. Vis. Exp.* **196**, e65052 (2023).

15. E. Villa *et al.*, Opening windows into the cell: Focused-ion-beam milling for cryo-electron tomography. *Curr. Opin. Struct. Biol.* **23**, 771–777 (2013).
16. J. Harapin *et al.*, Structural analysis of multicellular organisms with cryo-electron tomography. *Nat. Methods* **12**, 634–636 (2015).
17. V. Lucic, A. Leis, W. Baumeister, Cryo-electron tomography of cells: Connecting structure and function. *Histochem. Cell Biol.* **130**, 185–196 (2008).
18. B. Waugh *et al.*, Three-dimensional deconvolution processing for STEM cryotomography. *Proc. Natl. Acad. Sci. U.S.A.* **117**, 27374–27380 (2020).
19. M. Croxford *et al.*, Entropy regularized deconvolution of cellular cryo-transmission electron tomograms. *Proc. Natl. Acad. Sci. U.S.A.* **118**, e210873811 (2021).
20. M. Elbaum *et al.*, A proposed unified interphase nucleus chromosome structure: Preliminary preponderance of evidence. *Proc. Natl. Acad. Sci. U.S.A.* **119**, e2119101119 (2022).
21. Slinky, en.wikipedia.org. Accessed 1 May 2024.
22. J. Sedat *et al.*, A proposed unified mitotic chromosome architecture. *Proc. Natl. Acad. Sci. U.S.A.* **119**, e2119107119 (2022), https://doi.org/10.1073/pnas.2119107119.
23. Human_genome, en.wikipedia.org. Accessed 1 May 2024.
24. M. Noll, Subunit structure of chromatin. *Nature* **251**, 249–251 (1974).
25. A. Valouev, Determination of nucleosome organization in primary human cells. *Nature* **474**, 519 (2011).
26. Cytogenetics, en.wikipedia.org. Accessed 1 May 2024.
27. en.wikipedia.org/wiki/Chromosome_10. Accessed 1 May 2024.
28. N. Walther *et al.*, A quantitative map of human Condensin provides new insights into mitotic chromosome architecture. *J. Cell Biol.* **217**, 2309–2328 (2018).
29. E. Therman, *Human Chromosomes Structure Behavior Effects* (Springer-Verlag, ed. 2, 1985).
30. C. Erdönmez, "n-tuple complex helical geometry modeling using parametric equations. *Eng. Comput.* **30**, 715–726 (2014).
31. Finite_element_method, en.wikipedia.org. Accessed 1 May 2024.
32. comsol-multiphysics, www.comsol.com. Accessed 1 May 2024.
33. Promoter_(genetics), en.wikipedia.org. Accessed 1 May 2024.
34. Enhancer_(genetics), en.wikipedia.org. Accessed 1 May 2024.
35. W. Lai, B. Pugh, Understanding nucleosome dynamics and their links to gene expression and DNA replication. *Nat. Rev. Mol. Cell Biol.* **18**, 548–562 (2017), 10.1038/nrm.2017.47.
36. D. Goffney *et al.*, Controls of nucleosome positioning in the human genome. *PLoS Genet.* **11**, e1003036 (2012), 10.1371/jounal.pgen.1003036.
37. N. Abdulhay *et al.*, Massively multiplex single-molecule oligonucleosome footprinting. *eLife* **9**, e59404 (2020).
38. T. Cremer, C. Cremer, Chromosome territories, nuclear architecture and gene regulation in mammalian cells. *Nat. Rev. Genet.* **2**, 292–301 (2001).
39. Chromosome_territories, en.wikipedia.org. Accessed 1 May 2024.
40. T. Sexton *et al.*, Three-dimensional folding and functional organization principles of the *Drosophila* genome. *Cell* **148**, 458–472 (2012).
41. M. Pouokam *et al.*, The Rabl configuration limits topological entanglement of chromosomes in budding yeast. *Sci. Rep.* **9**, 6795 (2019).
42. D. Mathog, M. Hochstrasser, Y. Gruenbaum, H. Saumweber, J. Sedat, Characteristic folding pattern of polytene chromosomes in *Drosophila* salivary gland nuclei. *Nature* **308**, 414–421 (1984).
43. Y. Gruenbaum *et al.*, Spatial organization of the *Drosophila* nucleus: A three-dimensional cytogenic study. *J. Cell Sci. Suppl.* **1**, 223–234 (1984).
44. D. Mathog, M. Hochstrasser, J. Sedat, Light microscope-based analysis of three-dimensional structure: Applications to the study of *Drosophila* salivary gland nuclei. Part I: Data collection and analysis. *J. Microsc.* **137**, 241–252 (1984).
45. M. Hochstrasser *et al.*, Spatial organization of chromosomes in the salivary gland nuclei of *Drosophila melanogaster*. *J. Cell Biol.* **102**, 112–123 (1986).
46. M. Hochstrasser, J. Sedat, Three-dimensional organization of *Drosophila melanogaster* interphase nuclei. I. Tissue-specific aspects of polytene nuclear architecture. *J. Cell Biol.* **104**, 1455–1470 (1987).
47. M. Hochstrasser, J. Sedat, Three-dimensional organization of *Drosophila melanogaster* interphase nuclei. II. Chromosome spatial organization and gene regulation. *J. Cell Biol.* **104**, 1471–1483 (1987).
48. Eukaryotic_DNA_replication, en.wikipedia.org. Accessed 1 May 2024.
49. B. Alberts *et al.*, *Molecular Biology of the Cell* (Garland Science, ed. 6, 2014).
50. I. Attali, M. Bochan, J. Berger, Structural mechanisms for replicating DNA in eukaryotes. *Annu. Rev. Biochem.* 90, 77–106 (2021).
51. J. Urban, R. Ranjan, X. Chen, Asymmetric histone inheritance: Establishment, recognition, and execution. *Annu. Rev. Genet.* **56**, 113–43 (2022).
52. Cohesin, en.wikipedia.org. Accessed 1 May 2024.
53. T. G. Gligoris *et al.*, Closing the cohesin ring: Structure and function of its Smc3-kleisin interface. *Science* **346**, 963–967 (2014).
54. A. Cuadrado, A. Losada, Specialized functions of cohesins STAG1 and STAG2 in 3D geneome architecture. *Curr. Opin. Genet. Dev.* **61**, 9–16 (2020).
55. K. Nasmyth *et al.*, What AlphaFold tells us about Cohesin's retention on and release from chromosomes. *eLife* **12**, RP88656 (2023), 10.7554/eLife.88656.1.
56. Centromere, en.wikipedia.org. Accessed 1 May 2024.
57. Cell_cycle, en.wikipedia.org. Accessed 1 May 2024.
58. K. Luger *et al.*, Crystal structure of the nucleosome core particle at 2.8A resolution. *Nature* **389**, 251–260 (1997).
59. https://en.wikipedia.org/wiki/Condensin. Accessed 1 May 2024.
60. B.-G. Lee *et al.*, Cryo-EM structures of holo condensin reveal a subunit flip-flop mechanism. *Nat. Struct. Mol. Biol.* **27**, 743–751 (2020).
61. P. G. de Gennes, *Introduction to Polymer Dynamics* (Cambridge University Press, 1990), vol. 1.
62. W. Coffey, Yu. Kalmykov, J. Waldron, *The Langevin Equation* (World Scientific Publishing Co. Pte., Ltd., ed. 2, 2004).
63. A. Larson *et al.*, Liquid droplet formation by HP1α suggests a role for phase separation in heterochromatin. *Nature* **547**, 236–238 (2017).
64. H. Zhang *et al.*, Heterochromatin organization and phase separation. *Nucleus* **14**, 2159142 (2023).
65. P. Kirchweger, D. Mullick, P. P. Swain, S. G. Wolf, M. Elbaum, Correlating cryo-super resolution radial fluctuations and dual-axis cryo-scanning transmission electron tomography to bridge the light-electron resolution gap. *J. Struct. Biol.* **215**, 107982 (2023).
66. J. W. Sedat, L. Manuelidis, A direct approach to the structure of eukaryotic chromosomes. *Cold Spring Harb. Symp. Quant. Biol.* **42**, 331–350 (1978).
67. W. Beermann, "Chromosomes and genes" in *Results and Problems in Cell Differentiation. Developmental Studies on Giant Chromosomes*, W. Beermann, Ed. (Springer, Berlin, Germany, 1972), vol. 4, pp. 1–33.
68. I. F. Zhimulev *et al.*, Genetic organization of interphase chromosome bands and interbands in *Drosophila melanogaster*. *PLoS ONE* **9**, e101631 (2014).
69. K. P. Eagen, T. A. Hartl, R. D. Kornberg, Stable chromosome condensation revealed by chromosome conformation capture. *Cell* **163**, 934–946 (2015).
70. T. Y. Zykova, V. G. Levitsky, E. S. Belyaeva, I. F. Zhimulev, Polytene chromosomes--A portrait of functional organization of the *Drosophila* genome. *Curr. Genomics* **19**, 179–191 (2018).
71. L. L. Hua, T. Mikawa, Mitotic antipairing of homologous and sex chromosomes via spacial restriction of the two haploid sets. *Proc. Natl. Acad. Sci. U.S.A.* **115**, E12235–E12244 (2018).
72. P. Cai *et al.*, Ipsilateral restriction of chromosome movement along a centrosome, and apical-basal axis during the cell cycle. bioRxiv [Preprint] (2024). https://doi.org/10.1101/2023.03.27.534352; https://www.biorxiv.org/content/10.1101/2023.03.27.534352v1. Accessed 1 May 2024.
73. en.wikipedia.org/wiki/Wolfram Mathematica. Accessed 1 May 2024.